Pergamon

Journal of Structural Geology, Vol. 19, Nos 3-4, pp. 293 to 301, 1997
Published by Elsevier Science Ltd
Printed in Great Britain
0191-8141/97 $17.00 + 0.00

PII: S0191-8141(96)00102-2

Low-amplitude evolution of break-thrust folding

NICHOLAS B. WOODWARD

ER-15, Office of Energy Research, U.S. Department of Energy, 19901 Germantown Road, Germantown, MD 20874, U.S.A.

(*Received* 1 *February* 1996; *accepted in revised form* 11 *November* 1996)

Abstract—This paper proposes a mechanistic explanation for fault-related, flexural-slip folds that form predominantly by fixed-hinge folding (i.e. break-thrust folds). It also presents a stepwise evolutionary history for these folds which contrasts with the model suggested for self-similar, migrating-hinge, fault-propagation fold models. Both mechanical folding theory and rock-fabric evidence suggest that folding in advance of a growing thrust fault can evolve in a five-step process: (1) initial sinusoidal buckling instability (<2% permanent strain; <10° limb dips), (2) hinge migration from the symmetric buckling instability to an asymmetric kink geometry at very low strains (2–6% strain; 12°–20° forelimb dip) which is driven by interlayer shear stresses, (3) fold growth by limb rotation with fixed anticlinal and synclinal hinges, and propagation of a flat thrust beneath the fold (6–20% strain; 20°–35° forelimb dip), (4) fold locking caused by space problems and the inability to overcome the increasing angular shear required to continue flexural slip folding (20–36% strain; 35°–50° forelimb dip), and (5) partitioning of deformation accommodated by highly strained fold limbs, faulting on the flat basal décollement beneath the entire fold creating a detachment fold, or by continued faulting at the sub-fold ramp resulting in a fault breaking through the earlier fold. Published by Elsevier Science Ltd.

INTRODUCTION

This paper examines the constraints and requirements of the folding process that occurs in thrust belts. My approach contrasts with many recent discussions of thrust belt structures, which are based on the premise that fold geometries are entirely determined by fault shapes and amounts of slip on stepped faults (e.g. Rich, 1934; Suppe, 1983; Mitra, 1990; Suppe and Medwedeff, 1990). Both folding-dominated and faulting-dominated regions exist within thrust systems. I suggest an alternative description of the fold mechanisms in kink geometry, flexural-slip 'break-thrust' folding in thrust belts; and a kinematic/conceptual model analogous to that provided by Suppe (1983) and Suppe and Medwedeff (1990) for self-similar, migrating-hinge folding (called fault-propagation folds here) in thrust belts.

The common types of fault-related folds which form in advance of fault tips are fault-propagation folds, detachment folds, and break-thrust folds (Fig. 1). Most previous workers (e.g. Suppe, 1983; Jamison, 1987; Mitra, 1990; Groshong and Epard, 1994; Epard and Groshong, 1995; Homza and Wallace, 1995) have considered the geometries of fault-propagation and detachment folds without detailed discussion of rock deformation properties or mechanics.

As discussed by Fischer and Woodward (1990) and Woodward (1992), many thrust faults or thrust systems do not evolve with self-similar geometries, nor can 'typical' structural styles be tied to unique positions in a thrust system, as suggested by Elliott (1976) or Mitra (1990). This contribution considers what reasonable mechanical constraints can be added to our basic geometric models to improve our understanding of fold–thrust system evolution. The goal of this paper is to move beyond models solely supported by geometric similarities, to models which are also consistent with rock fabric data and mechanical understanding.

First, I will review the common fold geometries in thrust systems, and then the most common folding mechanisms proposed for flexural-slip folds. Additional constraints can be placed on folding models by field data and geometric checks on consistency (commonly called cross-section balancing). Finally, a new conceptual model is presented, which I believe is more representative of the conditions of folding present in many thrust-fault-related folds.

FUNDAMENTAL GEOMETRIES

Fault-related folds in foreland fold- and thrust-belts are dominated by flexural-slip parallel folding, although non-parallel folding may occur (represented by thickness changes during deformation) if strain is concentrated in limited areas of the structures. Suppe (1983) documented the relationship between fold interlimb angles and cut-off angles for parallel, fault-related folds and noted that there were two geometric solutions which fulfilled the criteria for parallel chevron-style folding above a stepped fault.

Mode I fault-bend folds have an open fold solution with interlimb angles of 130°–160°. Fold wavelengths for these type of folds are determined by the displacement of the ramp section onto the upper flat décollement zone (Rich, 1934) and the spacing of thrust ramps. Fold amplitude is determined by the thickness of the stratigraphic repetition at the ramp.

Mode II fault-bend folds have a tight interlimb angle solution (angles of 100°–60°) resulting in overturned

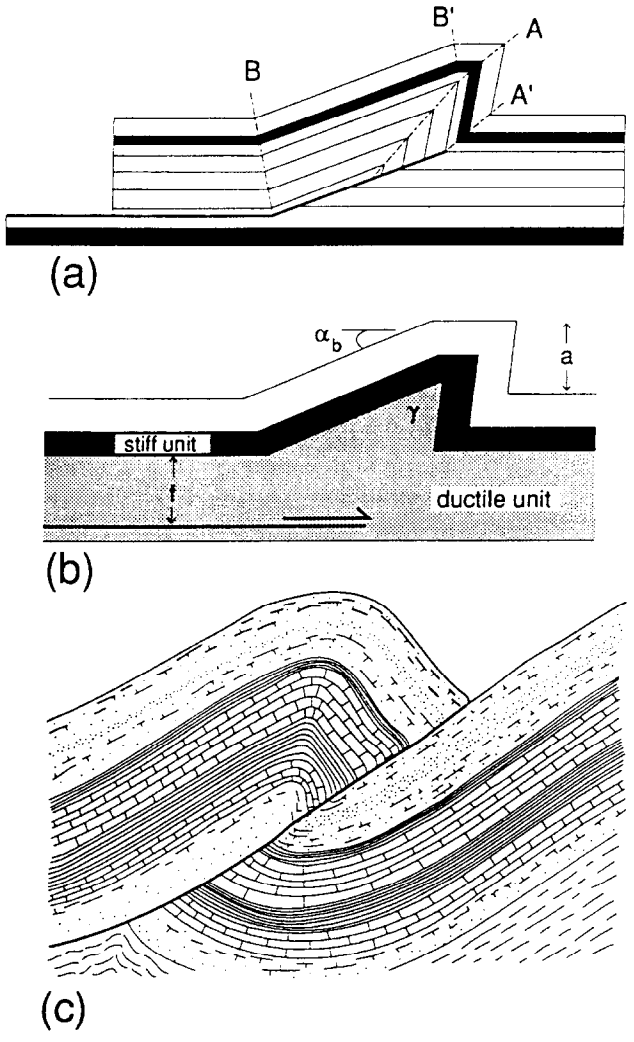

Fig. 1. Thrust-related fold models (after Suppe (1985), Jamison (1987) and Willis (1893), respectively): (a) fault propagation fold, (b) detachment fold, (c) break-thrust fold.

forelimbs in most cases. Suppe (1983) noted that most field examples exhibiting the Mode II geometry were fault-propagation folds, which grow during fault displacement by outward migration of fold hinges in advance of a ramping thrust fault (Suppe, 1983, 1985; Suppe and Medwedeff, 1990). Detachment folds (Dahlstrom, 1969, 1990; Jamison, 1987; Groshong and Epard, 1994; Epard and Groshong, 1995; Homza and Wallace, 1995) grow by folding above a décollement horizon, without a recognizable fault which steps upward. Break-thrust folds (Willis, 1893; Fischer *et al.*, 1992) begin as detachment folds and grow by folding with fixed hinges above and ahead of a propagating fault. Once the fold develops a close interlimb angle it locks, and will be cut by a ramping thrust.

Fault-propagation folds and break-thrust folds (both modeled and as reported in the field) are usually asymmetric towards the foreland (Jamison, 1987; Suppe and Medwedeff, 1990), and thus they cannot evolve into symmetric fault-bend folds. Ramp step-up angles are also quite different for parallel fault-bend and fault-propagation folding (Woodward *et al.*, 1989; Suppe and Medwedeff, 1990). Thus, fault-bend folds, fault-propagation folds, and break-thrust folds follow divergent deformation paths early in their history, contrary to many physical modelling studies (Chester and Chester, 1990; Chester *et al.*, 1991; Liu and Dixon, 1991, 1995; Dixon and Liu, 1991). Detachment folds may be either symmetric or asymmetric, and unless the basal detachment zone is fully observable, may be indistinguishable from fault-propagation folds or break-thrust folds.

FOLDING MECHANISMS

Single layer buckling

Buckling is common in single layers and multilayers. Theories and models which examine buckling are plentiful, usually for single layers (Biot, 1961, 1964, 1965a,b, 1967; Hudleston, 1973; Fletcher, 1974; Johnson, 1977, 1980; Latham, 1985a,b; Dixon and Tirrul, 1991; Dixon and Liu, 1991; Liu and Dixon, 1991, 1995; Lan and Hudleston, 1995 and many others). There are a number of mechanical results which are well established in the single layer studies: (a) incipient folding is preceded by $\pm 2\%$ elastic layer-parallel shortening (Johnson, 1980); (b) folds grow by amplification of initial randomly distributed perturbations, but amplification factors for different wavelengths differ within a single layer (Johnson, 1977); (c) when limb dips reach about 15°–20° (4–6% strain), wavelength selection effectively ceases and the final dominant wavelength grows rapidly (Biot, 1961; Chapple, 1968; Hudleston, 1973; Fletcher, 1974); (d) changes in single beam thicknesses lead to linear changes in dominant wavelength (Currie *et al.*, 1962; Ramsay, 1967; Fletcher, 1974; Hudleston and Lan, 1993, 1994); (e) although intrinsic anisotropy is important in defining layering and dominant wavelengths, anisotropy also can be induced by deformation partitioning into thin zones or 'mechanical bedding' (Latham, 1985a,b).

Multilayer buckling

It is much more difficult to define controlling parameters for multilayer buckle folds than for single layer folds because of the greater number of variables, such as the interlayer cohesion, material properties of individual layers, contrasts in the layer properties, and the bulk moduli of the multilayer package as a whole. Biot (1961) demonstrated that relatively simple multilayers can be treated in ways similar to single layers, as long as there are only two viscosity values for the different layers. The primary constraints then become the number of layers and the proportion of each type of layer. Experimental multilayer studies (Currie *et al.*, 1962; Johnson and Honea, 1975; Honea and Johnson, 1976; Weiss, 1980; Stewart and Alvarez, 1991) emphasize uniform layers and different degrees of bedding slip. In Currie *et al.*

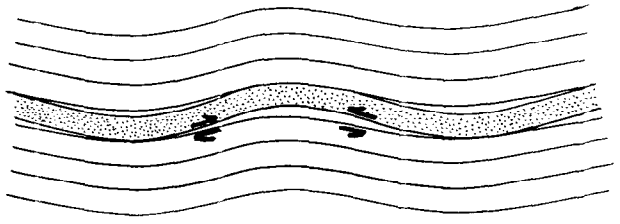

Fig. 2. The 5% thicker stippled competent unit has a longer dominant wavelength than that of the overall folding interval (after Ramsay, 1974). This causes extra interlayer shear towards the hinges during folding and space problems in fold cores.

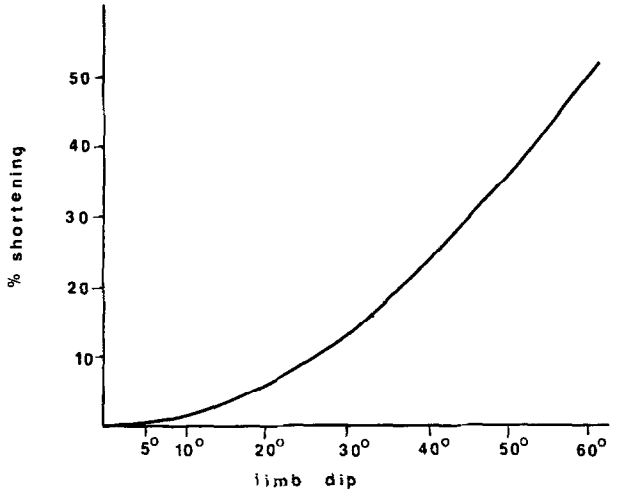

Fig. 3. Percent shortening plotted against angular rotation of fold limbs (based on the equation shortening $e = \cos$ limb dip $- 1$). By 50° limb dips (interlimb angle of 80°) when most parallel folds have locked, shortening increases at a constant rate with increasing limb dip.

(1962), the overall wavelength for a stratigraphic interval is determined by the dominant competent unit, and adjacent strata are forced to conform to that wavelength unless there is sufficient weak material separating different competent intervals.

The existence of multilayers in a natural stratigraphic section will create a number of competing dominant wavelengths during initial buckling, one for each competent stratigraphic interval. The wavelength selection process in different adjacent layers is in addition to the competing amplification rates of different potential wavelengths within an individual layer or interval (Fig. 2). Natural multilayers are highly variable in unit thicknesses and competencies. This is true both for restricted stratigraphic intervals such as individual 'structural lithic units' as defined by Currie *et al.* (1962) (see also Woodward and Rutherford, 1989), and for entire stratigraphic sections.

Flexural slip

Thrust-related folds commonly begin as flexural-slip parallel folds (Dahlstrom, 1969; Suppe, 1983). The strain rate of shortening that can be accommodated by limb rotation in folding is initially low, then increases until about 20% shortening has occurred, after which it decreases (Ramsay, 1974; Hardy and Poblet, 1994). This result is the combination of three elements: the amount of shortening accommodated by increments of limb rotation, space problems in the fold core, and the amount of angular shear required between layers to accommodate each increment of shortening.

The first 1% shortening requires 8° of limb rotation, the next 1% shortening requires only 4° of limb rotation, and after 3% shortening each additional 1% shortening requires less than 2° of limb rotation (Fig. 3). Limb rotation accommodates shortening effectively, however, only until space problems are encountered in the fold core at roughly 36% shortening (50° limb dip) (DeSitter, 1956; Ramsay, 1967).

Rates of shear strain between layers are high at low strains, decrease to a minimum at about 20% shortening (equivalent to a limb dip of 37°) and then increase rapidly (Ramsay, 1974).

Progressively less interlayer slip is needed to accommodate shortening from limb dips of 1° to 37° (strain softening). Beyond 37° limb dips, successively more interlayer slip is required for stable parallel folding (strain hardening).

Dominant wavelengths for buckle folding increase linearly with layer thickness (Currie *et al.*, 1962; Hudleston and Lan, 1993), thus thicker layers in multilayer folding will have longer dominant wavelengths than adjacent thinner layers of equal competence. The overall dominant wavelength for a multilayer interval will be longer than the initial 'ideal' dominant wavelength for some thinner competent layers, and will be shorter than the initial 'ideal' dominant wavelength for the thick layers. As shown in Fig. 2, the thicker units with slightly longer initial wavelengths in a multilayer interval introduce excess angular shear strain between those competent units and thinner adjacent ones. Angular shear between a thick competent layer and a surrounding interval of thinner competent layers will always be higher than that between equal thickness competent layers, but the difference, or 'excess' angular shear is largest at limb dips below 15° (Fig. 4). Of particular interest is that in the first 1% permanent strain (below 8° limb dip), the excess angular shear strain is much higher even if the dominant wavelength of a slightly thicker competent layer is only 1% longer than for the interval as a whole.

Kinking

Fault-related folds commonly have kink geometries which indicate the importance of kinking as well as buckling mechanisms (Dewey, 1966; Johnson, 1977; Weiss, 1980). Kink folds are commonly asymmetric parallel folds where most slip occurs on bedding in the limb between the hinges (kink band boundaries).

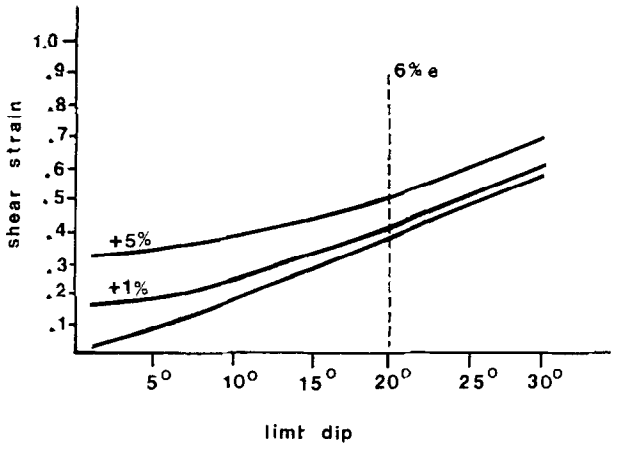

Fig. 4. The average shear strain parallel to layering within a chevron fold can be calculated from:

Angular shear strain between layers = tan limb dip
(from Ramsay, 1974).

Angular shear between layers for uniform layer thickness is plotted in the lowest line. The middle line plots the average angular shear between a 1% thicker competent unit (with a 1% longer dominant wavelength) and the adjacent beds in the folding interval. The upper lines plots the average angular shear between a 5% thicker competent unit (with a 5% longer dominant wavelength) and the adjacent beds in the folding interval. Excess angular shear is greatest at low limb dips, and becomes a small constant increment to the total average angular shear by 20° limb dip.

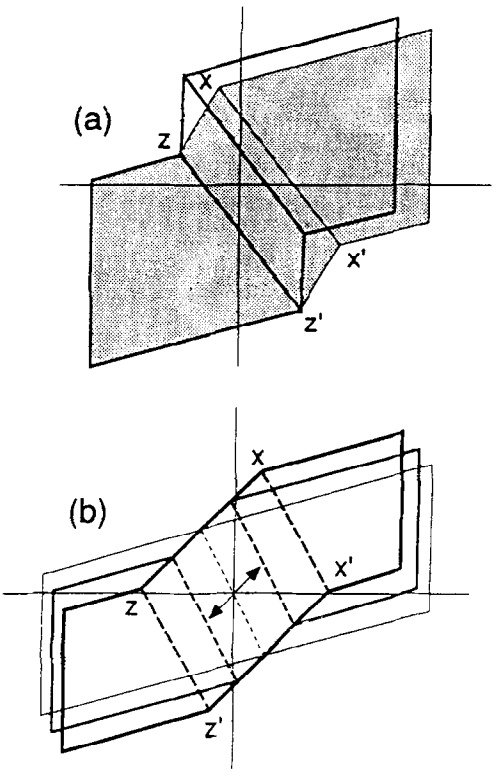

Fig. 5. Two end-members of ideal kink-fold kinematics. (a) Fixed-hinge kink evolves by progressive limb rotation until it locks because of space problems in the fold cores. (b) Migrating-hinge kink evolves by initial rapid formation of a narrow kink with final interlimb angle, and lateral movement of hinges x–x' and z–z' as shown by double-headed arrow. Modified from Weiss (1980).

Although ideal kinks are flexural-slip, parallel folds, dilation between beds within the kink band boundary is common (Dewey, 1966; Weiss, 1980; Stewart and Alvarez, 1991). Kink folds typically initiate from sinusoidal fold patterns, although the initial sinusoidal perturbation may be hardly visible when kinking begins (Johnson, 1977). Honea and Johnson's (1976) experiments suggested that strata with moderate contact strength boundaries exhibited kink folding once interlayer slip began, whereas strata with very weak layer boundaries exhibited sinusoidal-to-concentric folding. Latham (1985a,b) similarly argued that partitioning or localization of slip on a few layers (induced) anisotropy would drive kink folding, whereas high intrinsic anisotropy (uniform layer slip on many layers) encouraged concentric folding deformation.

End-member kink folds form either solely by initiation of a small kink band with close interlimb angles and hinges that migrate outward, or solely by limb rotation with fixed hinges until the fold locks, similar to buckle folds (Fig. 5; Dewey, 1966; Weiss, 1980). These two types of kink mechanisms parallel the distinctions between the simplest models of migrating-hinge fault-propagation folds and fixed-hinge break-thrust folds (Suppe and Medwedeff, 1990; Fischer *et al.*, 1992).

Kinks also may evolve by both limited hinge migration and limb rotation as proposed by Johnson (1977) and Stewart and Alvarez (1991). Johnson (1977) suggests, based on theoretical models, that final kink-fold geometries result from the superposition of a sinusoidal perturbation and an amplifying linear perturbation which produce a narrowing kink band as shortening increases, and that the layering yields at two hinges rather than by curving the entire layer (Fig. 6).

Stewart and Alvarez (1991) propose a migrating-hinge kink folding mechanism and suggest that the deformation style changes with increasing shortening. Their kink-band models nucleate at about 2.5% strain (13° limb dip). At low strains (2.5–10% strain) kink bands with gently curved hinges expand by outward hinge migration. From 10–35% strain (limb dips of 26°–49°) kinks continue to

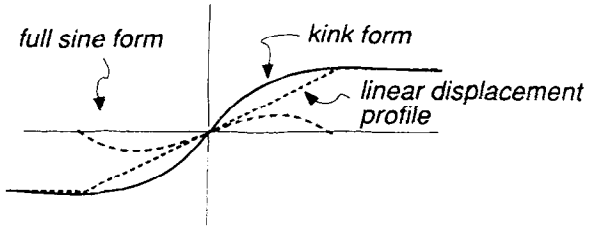

Fig. 6. Kink geometry presented by Johnson (1977). Kink form results from combination of full sine wave and linear displacement profile of a kink. The kink form may be smoothly curved or have sharp hinges. It forms by buckling followed by incomplete plastic yielding at the hinges located by the maximum bending moment.

expand by slower hinge migration and hinges sharpen until folds lock.

FIELD DATA

Fischer *et al.* (1992), Fisher and Anastasio (1994), and Homza and Wallace (1995) presented field data on geometries and rock fabrics strongly suggesting the existence of distinct fixed-hinge fault related folds separate from migrating-hinge fault-propagation folds as identified by Suppe and Medwedeff (1990). Fault-bend folds and many open buckle folds (160° to 140° interlimb angles) show little systematic fabric development uniquely related to hinge positions (Ramsay, 1967; Wiltschko *et al.*, 1985), suggesting that early open hinge locations probably cannot be uniquely identified later in folding if hinges migrate. Hedlund *et al.* (1994) report field data from slightly less open (130°–145° interlimb angles), curved, thrust-related folds which shows fixed-hinge folding based on growth patterns of antitaxial fibrous overgrowths and veins. Mitchell and Woodward (1988), Fischer *et al.* (1992), and Fisher and Anastasio (1994) all report field data showing typical hinge fabrics are lacking from either fold forelimbs or backlimbs in tighter folds. The accumulation of strain in fold hinges is a function of the strain rate and tightness of those hinges, but the mentioned field evidence suggests that fold-hinge migration will leave evidence once the interlimb angle is reduced to $\pm 140°$ or less. The sequence of microstructures in the forelimbs, and to a much lesser extent, in the backlimbs of fault-related folds frequently reflects initial layer parallel shortening (selvages and wedge faults), overprinted by extension features in variable orientations (vein systems), shear between layers, and frequently final shortening perpendicular to bedding (Mitchell and Woodward, 1988; Fischer *et al.*, 1992).

CROSS-SECTION BALANCE

Line length and area balancing of cross-sections has demonstrated that detachment folds have space problems (insufficient area and line length) in their cores as they are usually depicted (Dahlstrom, 1990; Groshong and Epard, 1994; Epard and Groshong, 1995; Homza and Wallace, 1995). The usual constraints on detachment folds are limb geometry and depth to detachment, and the suggested solutions to the balancing problems are to change the amount of material at the base of the structure (changing the depth to the detachment fault; Homza and Wallace, 1995), or to change the bed lengths within the structure by migrating hinges (Dahlstrom, 1990) or by strain (Jamison, 1987; Groshong and Epard, 1994; Epard and Groshong, 1995). Both Epard and Groshong (1995) and Homza and Wallace (1995) note that increasing fold asymmetry reduces the balancing problem by reducing the space problem at depth.

CONCEPTUAL MODEL

I am hesitant to offer another model for fault-related tip folds, but the evolution of predominantly fixed-hinge fault-related folds is hard to visualize without a stepwise geometric model. Idealized geometries (planar detachments, tight angular hinges, parallel straight layering), however, all maximize potential problems in creating a 'balanced model.' Figure 7 is based on five premises: (1) fixed depth of basal detachment; (2) preservation of the initial 5° limb dip in the datum horizon beneath the fold as a proxy for natural irregularities in layering and basal detachment; (3) conservation of key bed length (upper stratum in each diagram); (4) area change limited to less than 7%; and (5) limited inward hinge migration bounding the forelimb. Deformation is concentrated in the forelimb (area in x–y–z triangle) and no deformation is allowed in the leading syncline to the right of line y–z. The trailing synclinal axis is fixed beneath the detachment, but material is displaced forward through it (between U and T) to compensate for the forward motion of the key bed as the fold and thrust grow. The model can be compared with more idealized ones presented by Epard and Groshong (1995) and Homza and Wallace (1995).

The balanced and very simplified models preserve the leading syncline undeformed after its initial 0.4% background strain. They have non-parallel folding in the anticline with bed lengths shortening about 10% in the forelimb (triangle x–y–z). Although drawn as having uniform shortening and thickening, the forelimb shape change could be accommodated through any of several mechanisms such as wedge faulting, bulk strain, or minor folding. The backlimb is constrained by its length (line w–z–x–t is constant), and the return of its trailing edge to the regional level. The backlimb thickens from 0 to 10% from the trailing synclinal axis to the anticlinal hinge. Above a 20° forelimb dip, the lowest marker unit in the forelimb changes shape and thickens significantly in the model reflecting the need for increasing strain at depth to satisfy line length and area constraints (Epard and Groshong, 1995). Ramping of a thrust up from the detachment (Fig. 7e) is the preferred shortening mechanism after 30° forelimb dip.

DISCUSSION

Fischer *et al.* (1992) used field studies to support the Johnson (1977) model of a sinusoidal fold narrowing to a kink fold, but provided little discussion of the driving mechanisms or evolutionary steps in the transition. In the initial sinusoidal buckling of a uniform multilayer, interlayer shear will be greatest at the inflection points, but constant between beds. In initial buckling of a non-uniform multilayer, excess angular shear will be concentrated between competent layers of different thicknesses and will be greatest at low limb dips. As a result, natural

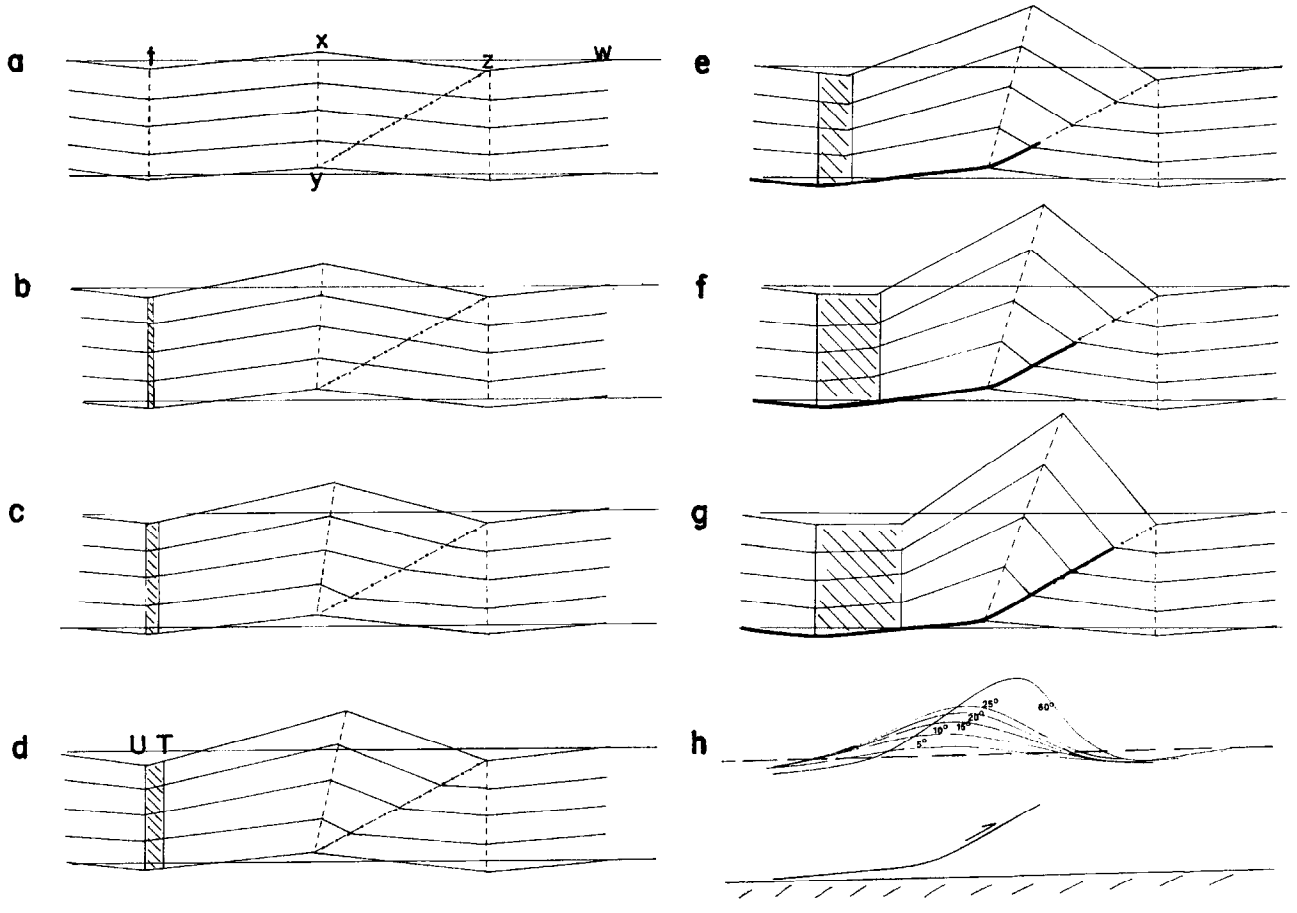

Fig. 7. Stepwise evolutionary model of an asymmetric, predominantly fixed-hinge, break-thrust fold. Line lengths and fold limb dips are measured on top-most key bed. Lowest folded surface with 5° limb dips is preserved as the base of deformation throughout the folding. Parallel upper and lower datum horizons shown for reference only. Synclinal hinges ahead and behind fold remain fixed in position and geometry with respect to lowest slightly folded boundary, although layering passes through trailing synclinal hinge into the backlimb of the anticline shown by hachured area (between *U* and *T*). With the slightly irregular basal surface, area is conserved between the undeformed- and deformed-state cross-sections within 7%, a value which would be very hard to document in the field. Table 1 summarizes geometric data. (a) Initial fixed-hinge symmetric fold with limb dips of 5°. (b) Fixed-hinge symmetric fold with 10° limb dips in key bed. (c) Inward-migrating hinge; forelimb shortens 6.5% in model with 15° forelimb dip of key bed. (d) Inward-migrating hinge; forelimb shortens additional 6.5% in model with 20° forelimb dip on key bed. (e) Fixed-hinge asymmetric fold with 30° forelimb dip on key bed, thrust ramp begins to grow parallel to *y*–*z* (although it may step up anywhere in forelimb); viable and admissible balanced models of evolving kink detachment-style folds suggest that additional material is needed to fill the uplift created by fold growth after 30° forelimb dips. (f) Fixed-hinge asymmetric fold with 40° forelimb dip on key bed and ramping thrust. (g) Fixed-hinge asymmetric fold with 50° forelimb dip and ramping thrust that reaches key bed. (h) More realistic synoptic kinematic evolution of a sinusoidal buckle fold into an asymmetric break-thrust fold with a kink-detachment fold geometry. The crest and trough of the fold migrate inwards at low limb dips to the stable kink morphology.

multilayers will tend to delaminate along competent unit boundaries at low limbs dips ($<10°$ and only 1% strain (Ramsay, 1967, 1974). This induced anisotropy provides a simple driving mechanism for the sinusoidal-to-kink fold growth sequence in a parallel folding sequence. Asymmetric folding accommodates fold growth with a constant detachment depth better than symmetric folding (Epard and Groshong, 1995; Homza and Wallace, 1995). The asymmetry of stress inherent in the thrusting environment (Hafner, 1951; Hubbert and Rubey, 1959; Goff and Wiltschko, 1992) should also contribute to the amplification of foreland-vergent kinking as the dominant fold form associated with foreland vergent thrusting.

After initial buckling and the beginning of the transition to a kink geometry, folding can take several paths: one is toward fault-propagation folding with a small, uniformly tight kink located over the tip of a flat detachment growing by outward hinge migration in association with a propagating thrust as it simultaneously steps upward; the second is toward a detachment fold with penetrative bulk strain at depth, perhaps with a changing depth to detachment; the third is toward detachment folding followed by break-thrust folding, with amplification of an asymmetric kink fold from the initial sinusoidal perturbation with growth mostly by limb rotation over a ramping thrust.

In the model proposed here, the fold grows asymme-

Table 1. The geometry in Fig. 7 is based on a slightly irregular initial geometry (preservation of initial 5° limb dips for substrate throughout the evolution of the structure). The geometry is highly simplified to illustrate major points. Line length shortening is concentrated in the forelimb in the model geometry by design between 10° and 20° limb dip. Overall area changes are less than 7%. Shortening calculation is based on a symmetric fold with designated limb dip using [shortening = cos limb dip − 1]. Asymmetric folds have slightly lower shortening for each forelimb dip

Shortening	Forelimb dip	Forelimb length change	Backlimb dip	Area change
0.015%	1°	0	1°	0
0.38%	5°	0	5°	0
1.5%	10°	0	10°	1.1%
3.4%	15°	7%	12.5°	2.3% +
6%	20°	13%	15.5°	4.5% +
9.1%	25°	0	19°	6.4% +
13.4%	30°	0	22°	6.8% +
23.4%	40°	0	28°	5.3% +
35.7%	50°	0	35°	1% +

trically from an initial sinusoidal perturbation (Fig. 7h). A detachment zone propagates laterally beneath the fold throughout the growth of the initial sinusoidal buckle fold to separate deforming strata from undeformed strata. The hinges migrate inward as suggested by Johnson (1977) up to limb dips of about 20° (140° interlimb angle). As discussed, field data suggest that fold-hinge migration has to be strictly limited beyond 20° limb dips. Kink folding with less than an ideal buckling wavelength is also supported by Fischer *et al.* (1992) who calculated buckling wavelengths for reasonable competent intervals in a number of thrust-related folds and found them to be systematically greater than observed forelimb lengths.

Fold amplification varies in magnitude along the length of the layer. Migration of symmetric open hinges inward towards an asymmetric shape occurs during fold growth from the initial perturbation both for the anticline and the syncline. From 0° to 20° forelimb dip (0–6% strain) the fold wavelength narrows as the layer yields at somewhat less than the initial sinusoidal dimension. From 20° to 50° forelimb dip (6–36% strain), hinges are fixed and fold growth occurs by limb rotation alone. Beyond 30° limb dips, detachment folds with flat décollements have space problems (i.e. material needs to move into the core to accommodate further uplift). In break-thrust folds, the basal fault required by the early detachment fold steps up to accommodate this space issue.

The maximum strain rate accommodated by folding occurs at 20–22% strain (36°–40° limb dip) and decreases at higher dips because of space problems in the fold core. In addition, the amount of angular shear between layers needed to accommodate further limb rotation also increases greatly above 36° limb dips. Above limb dips of 36°, therefore, the folds become progressively strain hardened. Faulting always is a competitive deformation mechanism, and the probability of continued faulting increases as the folds strain-harden, particularly by growth of new faults beneath the fold, or by growth of those which have stepped up into the core.

Instabilities of three different types dominate the evolution of fault-related folds: ramp failure; folding with thrusting (fault-propagation folds/break-thrust folds); and detachment folding without a ramping thrust. Each type of instability leads to a different deformation path. Multilayer anisotropy is a major variable in each of the instabilities, and the starting point for all of the deformation paths is compression and initial buckling of the layered sequence. The first and last competitive instabilities are those of folding versus faulting. Within the first 2% permanent strain, sinusoidal buckling dominates over other shortening mechanisms. The periodic spacing of thrust ramps locally and regionally, and the observation that ramps appear more closely spaced in thinner stratigraphic sections suggests that there may be 'wavelength' selection in ramp spacing (Goff *et al.*, 1990; Goff and Wiltschko, 1992; Liu and Dixon, 1995). Significant excess angular shear strain will be imposed on the limbs of the incipient folds and delamination between competent intervals has begun by 2% strain (12° limb dip). If the delamination is sufficiently extensive, the most competent interval will be separated from adjacent strata and may fail to create a ramp. Fundamental cut-off angles for ramps are in the range of 10°–20° (Suppe, 1983). Thus ramp failure at 2% buckling strain by faulting parallel (±) to the basal décollement will give appropriately low cut-offs angles and will leave little evidence of any initial buckling amplitude.

Ramp failure will connect a lower décollement to the next higher delaminated zone. If the delamination is extensive (beyond a single wavelength) or propagates well ahead of the ramp, a duplex may result from successive ramp formation between upper and lower delamination zones. The regular length spacing of duplex horses has suggested to many authors (e.g. Goff *et al.*, 1990; Hedlund *et al.*, 1994; Liu and Dixon, 1995) that sinusoidal folding perturbations predict horse length, fabric evolution, and fault breakthrough in forelimb positions. Many 'single-bed' duplexes also probably reflect this delamination. Single bed duplexes on large-scale limbs of folds and along flats clearly accommodate this type of shear between competent layers or structural units.

CONCLUSIONS

The purpose of this contribution is to develop a mechanistically constrained evolutionary model for the kinematic development of asymmetric, kink-geometry, fault-related folds consistent with rock fabric evidence and the conservation principles of line-length and cross-sectional area. The courses of future deformation paths are probably determined within the first 6% strain (20°

limb dip). By this time, wavelength selection has occurred. Multilayers within a natural stratigraphic section will have different dominant wavelengths and will impose significant excess angular shear between competent intervals. The wavelength-selection and amplification-imposed angular shear will tend to delaminate the section as a function of the vertical positions of competent units. This delamination will enhance the formation of detachment horizons and ramp failure in some areas, and kink-folding from low-amplitude, sinusoidal, buckle folding in other areas. The transition from sinusoidal buckling to mobile-hinge kinks to fixed-hinge kinks is proposed to occur at low limb dips (0°–20°) by changing rates of fold amplification along a layer driven by the delamination, and by the foreland-vergent overall stress field.

Migration of open hinges (up to 20° limb dip) cannot be ruled out based on rock fabric evidence because open folds with low limb dips do not usually have penetrative fabric development concentrated at the hinges. After a 20° forelimb dip (140° interlimb angle) is reached, fold hinge positions are essentially fixed, and fold growth is driven by the high-strain rates accommodated by limb rotation. After 36° limb dips are reached (22% strain), the rate of shortening that can be accommodated with increased limb rotation decreases and the folds strain-harden. The growth of break-thrust folds beyond 30° forelimb dips requires migration of material beneath the growing fold to maintain viability and admissability, and therefore requires a thrust stepping up from the detachment.

I propose a deformation sequence during the growth of individual break-thrust folds that can be understood based on simple folding theory, and that suggests straight-forward causal reasons for the change-over from one fold form to another. Folding processes can be expected to be important even in thrust-faulted terrains, and will generate final geometries similar to those predicted by faulting-dominated models because both rely on parallel folding with locking angles determined by layer thicknesses.

Acknowledgements—I would like to acknowledge the many helpful discussions I have had on the subject of fault-related folding with many colleagues, and particularly Mark Fischer, Dave Anastasio, and Mike Mitchell. I would like to also thank Jim Evans for editorial assistance, and Dave McConnell, Eric Erslev and the other anonymous reviewers of this paper for their careful attention to detail.

REFERENCES

Biot, M. A. (1961) Theory of folding of stratified visco-elastic media and its implications in tectonics and orogenesis. *Geological Society of America Bulletin* **72**, 1595–1620.

Biot, M. A. (1964) Theory of internal buckling of a confined multilayered structure. *Geological Society of America Bulletin* **75**, 563–568.

Biot, M. A. (1965) Theory of similar folding of the first and second kind. *Geological Society of America Bulletin* **76**, 251–258.

Biot, M. A. (1965) Further development of the theory of internal buckling of multilayers. *Geological Society of America Bulletin* **76**, 833–840.

Biot, M. A. (1967) Rheological stability with couple stresses and its application to geological folding. *Proceedings of the Royal Society, London* **A298**, 402–423.

Chapple, W. M. (1968) A mathematical model of finite-amplitude rock folding. *Geological Society of America Bulletin* **79**, 47–68.

Chester, J. S. and Chester, F. M. (1990) Fault-propagation folds above thrusts with constant dip. *Journal of Structural Geology* **12**, 903–910.

Chester, J. S., Logan, J. M. and Spang, J. H. (1991) Influence of layering and boundary conditions on fault-bend and fault-propagation folding. *Geological Society of America Bulletin* **103**, 1059–1072.

Currie, J. B., Patnode, H. W. and Trump, R. P. (1962) Development of folds in sedimentary strata. *Geological Society of America Bulletin* **73**, 655–674.

Dahlstrom, C. D. A. (1969) The upper detachment in concentric folding. *Bulletin of Canadian Petroleum Geology* **10**, 326–346.

Dahlstrom, C. D. A. (1990) Geometric constraints derived from the law of conservation of volume and applied to evolutionary models for detachment folding. *Bulletin of the American Association of Petroleum Geologists* **74**, 336–344.

DeSitter, L. V. (1956) *Structural Geology*. New York, McGraw-Hill.

Dewey, J. (1966) Nature and origin of kink bands. *Tectonophysics* **1**, 459–494.

Dixon, J. M. and Liu S. (1991) Centrifuge modelling of the propagation thrust faults. In *Thrust Tectonics*, ed. K. R. McClay, pp. 53–70. Chapman and Hall, London.

Dixon, J. M. and Tirrul, R. (1991) Centrifuge modelling of fold–thrust structures in a tripartite stratigraphic succession. *Journal of Structural Geology* **13**, 3–20.

Epard, J.-L. and Groshong, R. H. (1995) Kinematic model of detachment folding including limb rotation, fixed hinges and layer parallel strain. *Tectonophysics* **247**, 85–103.

Elliott, D. (1976) The energy balance and deformation mechanisms of thrust sheets. *Philosophical Transactions of the Royal Society, London* **282**, 289–312.

Fisher, D. M. and Anastasio, D. J. (1994) Kinematic analysis of a large-scale leading edge fold, Lost River Range, Idaho. *Journal of Structural Geology* **16**, 337–364.

Fischer, M. P. and Woodward N. B. (1990) The geometric evolution of foreland thrust systems. In *Thrust Tectonics*, ed. K. R. McClay, pp. 181–189. Chapman and hall, London.

Fischer, M. P., Woodward, N. B. and Mitchell, M. M. (1992) The kinematics of break-thrust folds. *Journal of Structural Geology* **14**, 451–460.

Fletcher, R. C. (1974) Wavelength selection in the folding of a single layer with power-law theology. *American Journal of Science* **274**, 1029–1043.

Goff, D. and Wiltschko, D. V. (1992) Stresses beneath a ramping thrust sheet. *Journal of Structural Geology* **14**, 437–449.

Goff, D., Wiltschko, D. V. and Fletcher, R. C. (1990) Folding as a controlling influence on the location of fault ramps in thrust belts. *Geological Society of America Abstracts with Programs* **22**, A272.

Groshong, R. H. and Epard, J.-L. (1994) The role of strain in area-constant detachment folding. *Journal of Structural Geology* **16**, 613–618.

Hafner, W. (1951) Stress distribution and faulting. *Geological Society of America Bulletin* **62**, 373–398.

Hardy, S. and Poblet, J. (1994) Geometric and numerical model of progressive limb rotation in detachment folds. *Geology* **22**, 371–374.

Hedlund, C. A., Anastasio, D. J. and Fisher, D. M. (1994) Kinematics of fault-related folding in a duplex, Lost River Range, Idaho, U.S.A. *Journal of Structural Geology* **16**, 571–584.

Homza, T. X. and Wallace, W. K. (1995) Geometric and kinematic models for detachment folds with fixed and variable detachment depths. *Journal of Structural Geology* **17**, 575–588.

Honea, E. and Johnson, A. (1976) A theory of concentric, kink and sinusoidal folding and of monoclinal flexuring of compressible, elastic multilayers IV. *Tectonophysics* **30**, 197–239.

Hubbert, M. K. and Rubey, W. W. (1959) Role of fluid pressure in mechanics of overthrust faulting I. Mechanics of fluid-filled porous solids and its application to overthrust faulting. *Geological Society of America Bulletin* **70**, 115–166.

Hudleston, P. J. (1973) An analysis of 'single-layer' folds developed experimentally in viscous media. *Tectonophysics* **16**, 189–214.

Hudleston, P. J. and Lan, L. (1993) Information from fold shapes. *Journal of Structural Geology* **15**, 253–264.

Hudleston, P. J. and Lan, L. (1994) Rheological controls on the shapes of single-layer folds. *Journal of Structural Geology* **16**, 1007–1021.

Jamison, W. R. (1987) Geometric analysis of fold development in overthrust terranes. *Journal of Structural Geology* **9**, 207–219.

Johnson, A. M. (1977) *Styles of Folding*. Elsevier Scientific Publishing, Amsterdam.

Johnson, A. M. (1980) Folding and faulting of strain-hardening sedimentary rocks. *Tectonophysics* **62**, 251–278.

Johnson, A. M. and Honea, E. (1975) A theory of concentric, kink and sinusoidal folding and of monoclinal flexuring of compressible elastic multilayers III. *Tectonophysics* **25**, 261–280.

Lan, L. and Hudleston, P. J. (1995) The effects of rheology on the strain distribution in single layer folds. *Journal of Structural Geology* **17**, 727–738.

Latham, J.-P. (1985) The influence of non-linear material properties and resistance to bending on the development of internal structures. *Journal of Structural Geology* **7**, 225–236.

Latham, J.-P. (1985) A numerical investigation and geological discussion of the relationship between folding, kinking and faulting. *Journal of Structural Geology* **7**, 237–249.

Liu, S. and Dixon, J. M. (1991) Centrifuge modelling of thrust faulting: structural variation along strike in fold-thrust belts. *Tectonophysics* **188**, 39–62.

Liu, S. and Dixon, J. M. (1995) Localization of duplex thrust ramps by buckling: analog and numerical modelling. *Journal of Structural Geology* **17**, 875–886.

Mitchell, M. M. and Woodward, N. B. (1988) Kink detachment fold in the southwest Montana fold and thrust belt. *Geology* **16**, 162–165.

Mitra, S. (1990) Fault propagation folds: geometry, kinematic evolution, and hydrocarbon traps. *Bulletin of the American Association of Petroleum Geologists* **74**, 921–945.

Ramsay, J. G. (1967) *Folding and Fracturing of Rocks*. McGraw-Hill, New York.

Ramsay, J. G. (1974) Development of chevron folds. *Geological Society of America Bulletin* **85**, 1741–1754.

Rich, J. L. (1934) Mechanics of low-angle overthrust faulting illustrated by Cumberland thrust block, Virginia, Kentucky and Tennessee. *Bulletin of the American Association of Petroleum Geologists* **18**, 1584–1596.

Stewart, K. G. and Alvarez, W. (1991) Mobile-hinge kinking in layered rocks and models. *Journal of Structural Geology* **13**, 243–259.

Suppe, J. (1983) Geometry and kinematics of fault-bend folding. *American Journal of Science* **283**, 681–721.

Suppe, J. (1985) *Principles of Structural Geology*. Prentice-Hall, Englewood Cliffs, New Jersey.

Suppe, J. and Medwedeff, D. A. (1990) Geometry and kinematics of fault-propagation folding. *Eclogae Geologicae Helvetiae* **83**, 409–454.

Weiss, L. E. (1980) Nucleation and growth of kink bands. *Tectonophysics* **65**, 1–38.

Willis, B. (1893) Mechanics of Appalachian Structure. U.S. Geological Survey Annual Report **13** (1891–1892), part 2, 217–281.

Wiltschko, D. V., Medwedeff, D. A. and Millson, H. E. (1985) Distributions and mechanisms of strain within rocks on the northwest ramp of Pine Mountain block, southern Appalachian foreland: a field test of theory. *Geological Society of America Bulletin* **96**, 426–435.

Woodward, N. B. (1992) Deformation styles and geometric evolution of some Idaho–Wyoming thrust belt structures. In *Structural Geology of Fold and Thrust Belts*, eds S. Mitra and G. W. Fisher, pp. 191–206. Johns Hopkins Press, Baltimore.

Woodward, N. B. and Rutherford, E. (1989) Structural lithic units in external orogenic zones. *Tectonophysics* **158**, 247–267.

Woodward, N. B., Boyer S. E., and Suppe J. (1989) Balanced geological cross-sections: an essential technique in geological research and exploration. *American Geophysical Union, International Geological Congress. Short Course in Geology* **6**.